

# Visual Based Navigation of Mobile Robots

*Report submitted in partial fulfillment to the requirements  
for the degree of*

BACHELOR OF TECHNOLOGY

*by*

**SHAILJA**



**Department of Electrical Engineering**  
Indian Institute of Technology, Kharagpur  
West Bengal, INDIA 721302  
November 2015

# Certificate

This is to certify that the report entitled **Visual Based Navigation of Mobile Robots**, submitted by **Shailja**, an undergraduate student, in the *Department of Electrical Engineering, Indian Institute of Technology, Kharagpur, India*, for the award of the degree of Bachelor of Technology, is a record of the work carried out by her under our supervision and guidance. Neither this report nor any part of it has been submitted for any degree or academic award elsewhere.

**Dr. Jayanta Mukhopadhyay**

Professor,

Department of Computer Science and Engineering,

Indian Institute of Technology, Kharagpur,

INDIA 721302

# Contents

<b>1</b>	<b>Introduction</b>	<b>1</b>
1.1	Project Overview . . . . .	1
1.2	Challenges and Constraints . . . . .	2
<b>2</b>	<b>Obstacle Detection</b>	<b>3</b>
2.1	Overview . . . . .	3
<b>3</b>	<b>Superpixel Segmentation</b>	<b>5</b>
3.1	Introduction . . . . .	5
3.2	Benefits of superpixel over pixel . . . . .	5
3.3	Simple Linear Iterative Clustering (SLIC) . . . . .	6
3.3.1	SLIC segmentation algorithm . . . . .	6
3.3.2	Time Complexity . . . . .	7
<b>4</b>	<b>Preprocessing of Image</b>	<b>10</b>
4.1	Color Space . . . . .	10
4.1.1	RGB color space . . . . .	10
4.1.2	Lab color space . . . . .	11
4.2	Gaussian Kernel Smoothing . . . . .	12
<b>5</b>	<b>Histogram Sampling</b>	<b>14</b>
5.1	Accessing individual superpixel of segmented image . . . . .	14
5.2	Histogram . . . . .	15
5.2.1	Safe zone histogram sampling . . . . .	17
<b>6</b>	<b>Floor Segmentation</b>	<b>18</b>
6.1	Calculation of independent Variables . . . . .	18
6.2	Classification of Superpixel . . . . .	20
6.2.1	Experimental Results . . . . .	21
6.3	Problem . . . . .	23
6.4	Conclusions . . . . .	23
6.5	Other floor segmentation methods . . . . .	23
6.6	Floor Junction Masking . . . . .	24
6.7	Region Growing . . . . .	28

## CONTENTS

6.8 Results . . . . .	29
<b>7 Mapping the environment</b>	<b>30</b>
7.1 Overview . . . . .	30
7.2 Perspective Mapping . . . . .	30
7.2.1 Image Formation and Perspective Mapping . . . . .	30
7.2.2 Homogeneous Coordinates . . . . .	31
7.2.3 Homography . . . . .	31
7.3 Algorithm . . . . .	32
7.4 Test Platform . . . . .	34
<b>8 Future Work</b>	<b>35</b>
<b>9 Conclusion</b>	<b>36</b>
<b>Bibliography</b>	<b>37</b>

# Introduction

## 1.1 Project Overview

As humans, if a mobile robot has to get familiar with a completely unknown environment, it should be able to build the map of the environment by exploring it. Like us, Robots can map only a part of the environment which is visible from current position. It should be able to navigate autonomously and planning a safe obstacle free path to reach there. This finds applications in personal assistant robot which can carry out tasks thereby saving us time and improving the quality of our lives. Moreover, some tasks can be completed more effectively by a machine rather than a person. Life would be so much easier and richer with an intelligent personal robot in the house! In contrast to industrial robots, which are generally programmed to carry out a few fixed tasks, personal robots need to adapt to wide variety of human environments and carry out a diverse array of tasks, learning as they go. In light of this, we see that the basic skills of understanding the environment such as mapping and perception are critical for such robots.

It is quite a challenging task to develop such an autonomous system. [1] With improvements in technology and the vast amount of research being done in the field of robotics, a few mobile robots have already been built that utilize laser range finders as their primary sensor to operate. However, one of the major hurdles standing in the way of widespread household adoption is the cost. All these robots are very expensive and in general, most people will not be able to afford them.

In this project we are applying algorithms which can be helpful in obstacle free navigation by detecting real world co-ordinates and suitable window of advancement.

## 1.2 Challenges and Constraints

Autonomous robot navigation itself is a challenging task. On top of this, making one with just monocular vision seems to be a daunting task! Sonar sensors have low range and resolution while laser range finders offer good resolution and in general produce good quality point clouds. They provide reasonably accurate distance measurements and obstacle detection algorithms have been developed using this range data. Moreover, almost all of the existing Simultaneous Localization and Mapping (SLAM) [2] based algorithms rely on range data to function. Instead of expensive laser sensors, a stereo vision system can possibly be used to get the depth information by comparing the disparity between the left and right images. Two cameras are also much less expensive than a laser range finder. However, stereo vision systems have their own shortcomings. They often produce very sparse point clouds, require careful calibration, and moreover are computationally quite expensive (disparity map and optical flow calculation). The major shortcoming of monocular vision is the loss of this depth data since the points traced along a ray from the camera are mapped into one pixel. New methods need to be developed to either bypass this requirement, or to estimate the depth. One big advantage of vision is that it allows the robot to see and hence understand. With just a distance sensor it would be blind, in the sense that it would not be able to recognize most of the objects lying around. With the advancement in object detection research, this could become a real possibility using monocular vision.

# Obstacle Detection

Collision-free navigation, and hence obstacle detection, is a very important task for autonomous mobile robots. Typically, most robots rely on range data such as that from ultrasonic sensors, laser range finders or stereo vision to detect obstacles. These sensors, especially the laser range finder, produce good results. However, they have some major drawbacks. The laser range finder is expensive, and hence would not be suitable for consumer use or for light-weight robots. Ultrasonic sensors are cheaper, but they generally suffer from low angular resolution. Stereo vision based approaches are computationally expensive, generally produce a sparse point cloud and require precise calibration. Moreover, range data based approaches are unable to distinguish between different surfaces of the same height (e.g. between pavement and rocky areas in a park) or small/flat objects lying on the ground. So, with the advancement in vision algorithms in the recent years, a monocular vision based approach presents a good alternative. The key difference in monocular vision based obstacle detection and range data based obstacle detection is that in the former, obstacles are distinguished from the ground by their appearance, whereas in the latter, they are detected by the difference in their relative distance. We present a multi-stage method for obstacle detection.

## 2.1 Overview

The obstacle detection algorithm takes a single image from the robots camera feed, and determines which areas are traversable and which parts are obstacles. We have made the following assumptions for speed and simplicity:

- The area immediately in front of the robot is free of obstacles.
- All obstacles have their base on the ground, i.e. there are no hanging obstacles.

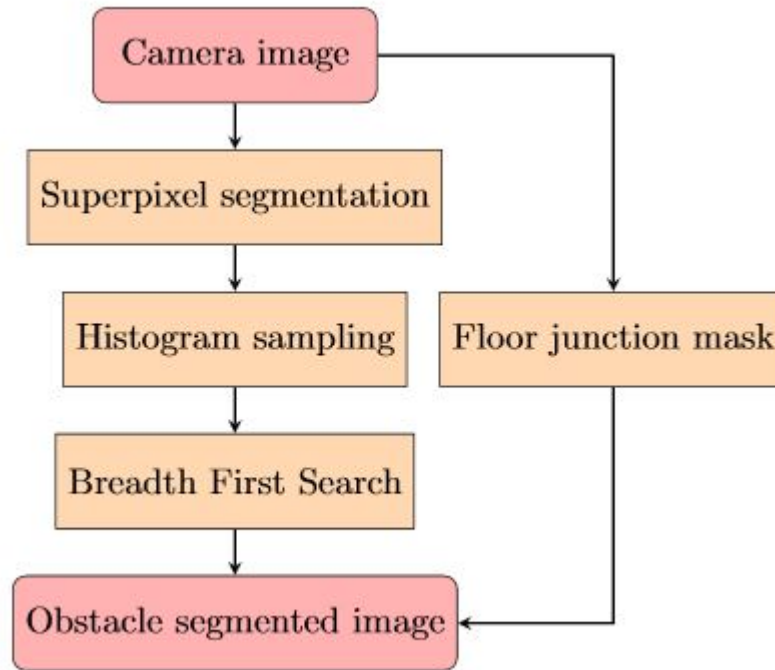


FIGURE 2.1: Block diagram of the obstacle detection process

- Robot motion is constrained to the horizontal ground plane.

The first step consists of segmenting the input image into superpixels, which are local groupings of similar pixels. Simple Linear Iterative Clustering is a fast algorithm used for finding the superpixels in an image. Superpixel segmentation allows the image to be processed as a set of regions, rather than a set of individual pixels, which speeds up the subsequent stages. The second step consists of histogram-based sampling. The superpixels that represent the immediate vicinity of the robot are sampled, and the color information is stored in a histogram. Next, we run a breadth first search over the superpixels, and classify regions as traversable or non-traversable in the process according to a membership criterion. Lastly, we estimate the floor junctions, where the obstacles meet the floor, from the camera image and use this to mask the final obstacle image. Fig. 2.1 shows a block diagram of the process.

# Supapixel Segmentation

## 3.1 Introduction

Generally, images are represented as grid of pixels but pixel is not the natural representation of image. Pixel does not carry any semantic meaning of the corresponding image but analysing a local group of pixels will give more meaning. This local grouping of pixels is called a superpixel.

## 3.2 Benefits of superpixel over pixel

- Computational efficiency: While it may be computationally expensive to compute the actual superpixel groupings, superpixel allows us to reduce the complexity of the images themselves from hundreds of thousands of pixels to only a few hundred superpixels. Each of these superpixels will then contain some sort of perceptual, and ideally, semantic value.
- Perceptual meaningfulness: Instead of only examining a single pixel in a pixel grid, which carries very little perceptual meaning, pixels that belong to a superpixel group share some sort of commonality, such as similar color or texture distribution.
- Oversegmentation: Superpixel algorithms oversegment the image. This means that most of important boundaries in the image are found; however, at the expense of generating many insignificant boundaries. The end product of this oversegmentation is that that very little (or no) pixels are lost from the pixel grid to superpixel mapping.

- Graphs over superpixel: Suppose if we want to represent an image as graph where each pixel represent a node and are related to other pixel through edges, this leads to a very complex representation with more number of pixels.

### 3.3 Simple Linear Iterative Clustering (SLIC)

We used SLIC algorithm for superpixel segmentation that clusters pixels in the combined five-dimensional color and image plane space to efficiently generate compact, nearly uniform superpixels. SLIC is simple to implement and easily applied in practice- the only parameter required is desired number of superpixels [3].

#### 3.3.1 SLIC segmentation algorithm

SLIC generates superpixels by clustering pixels based on their color similarity and proximity in the image. This can be done in five dimensional [rgbxy] space or [labxy] space, where [rgb] and [labxy] are the pixel vectors and xy is the pixel position. Superpixel size varies with the image size. It is not possible to simply use Euclidean distance in this 5D space without normalizing the spatial distances. A new distance measure that considers superpixel size is used which enforces color similarity as well as pixel proximity in this 5D space. For an image with N pixels, if we desire K superpixels, then approximate size of each superpixel will be N/K pixels and for roughly equally sized superpixels there would be a superpixel center at every grid interval  $S = \sqrt{(N/K)}$ .

For RGB color space:

$$d(p_1, p_2) = \sqrt{(r_1 - r_2)^2 + (g_1 - g_2)^2 + (b_1 - b_2)^2} + \frac{M}{S} \sqrt{(x_1 - x_2)^2 + (y_1 - y_2)^2} \quad (3.1)$$

For CIELAB color space:

$$d(p_1, p_2) = \sqrt{(l_1 - l_2)^2 + (a_1 - a_2)^2 + (b_1 - b_2)^2} + \frac{M}{S} \sqrt{(x_1 - x_2)^2 + (y_1 - y_2)^2} \quad (3.2)$$

A variable M is introduced to control compactness of superpixel. The greater the value of M,, the more spatial proximity is emphasized and more compact the cluster. we have chosen M=10. K regularly spaced cluster centers and moving them to seed locations corresponding to the lowest gradient position in 3 x 3 neighbourhood.

$$G(x, y) = \|I(x + 1, y) - I(x - 1, y)\|^2 + \|I(x, y + 1) - I(x, y - 1)\|^2 \quad (3.3)$$

where  $I(x,y)$  is the rgb or lab vector corresponding to the pixel at position  $(x,y)$ , and  $\|\cdot\|$  is the L2 norm. This takes into account both color and intensity information. Each pixel in the image is associated with the nearest cluster center whose search area overlaps this pixel. After all the pixels are associated with the nearest cluster center, a new center is computed as the average vector of all the pixels belonging to the cluster. We then iteratively repeat the process of associating pixels with the nearest cluster center and recomputing the cluster center until convergence. We enforce connectivity in the last step of our algorithm by relabeling disjoint segments with the labels of the largest neighboring cluster. We enforce connectivity in the last step of our algorithm by relabeling disjoint segments with the labels of the largest neighboring cluster. This step is  $O(N)$  complex and takes less than 10% of the total time required for segmenting an image.

---

**Algorithm 1** SLIC Superpixel segmentation
 

---

1. Initialize cluster centers  $C_k = [l_k, a_k, b_k, x_k, y_k]^T$  by sampling pixels at regular grid steps  $S$ .
  2. Perturb cluster centers in an  $nn$  neighborhood, to the lowest gradient position.
  3. **repeat**
  4.     **for** each cluster center  $C_k$  **do**
  5.         Assign the best matching pixels from a  $2S * 2S$  square neighborhood around the cluster center according to the distance measure (Eq. 1).
  6.     **end for**
  7.     Compute new cluster centers and residual error  $E$  L1 distance between previous centers and recomputed centers
  8. **until**  $E$  threshold
  9. Enforce connectivity.
- 

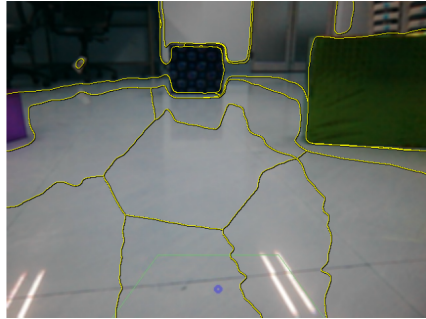
### 3.3.2 Time Complexity

By virtue of using our distance measure of Eq. (1), we are able to localize our pixel search on the image plane that is inversely proportional to the number of superpixels  $K$ . A pixel falls in the local neighborhood of no more than eight cluster centers. The convergence

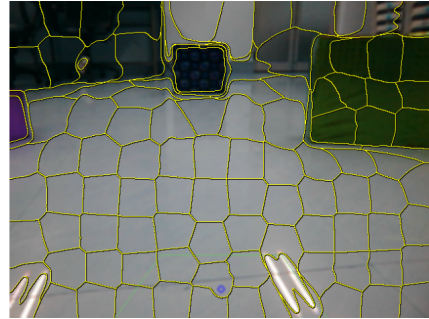
error of our algorithm drops sharply in a few iterations. The time complexity for the classical k-means algorithm is  $O(N KI)$  where  $N$  is the number of data points (pixels in the image),  $K$  is the number of clusters (or seeds), and  $I$  is the number of iterations required for convergence. But SLIC superpixel segmentation has time complexity of  $O(N)$  since we need to compute distances from any point to no more than eight cluster centers and the number of iterations is constant.



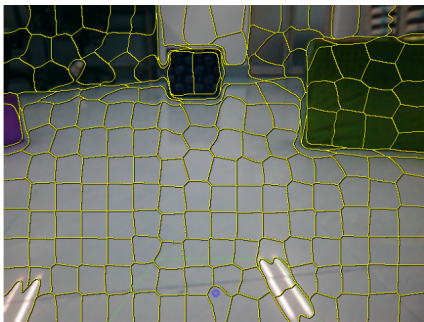
FIGURE 3.1: Camera Image



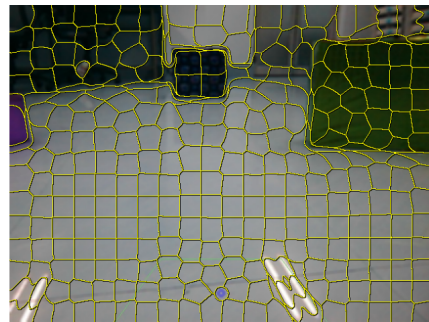
(a) K=10



(b) K=100



(c) K=200



(d) K=300

FIGURE 3.2: After applying SLIC superpixel segmentation

# Preprocessing of Image

## 4.1 Color Space

A color space is the type and number of colors that originate from the combinations of color components of a color model. A color model is an abstract configuration describing how color impression can be created, which consists of color components and rules about how these components interact.

SLIC superpixel segmentation was applied to RGB image and after converting it to lab color space.

### 4.1.1 RGB color space

RGB color space is defined by three chromaticities of red, green and blue primaries. Fig 4.1 shows the superpixel segmentation on RGB image.



FIGURE 4.1: Superpixel segmentation for  $K=200$  in rgb color space.

#### 4.1.2 Lab color space

A Lab color space is a color-opponent space with dimension  $L$  for lightness and  $a$  and  $b$  for the color-opponent dimensions, based on nonlinearly compressed coordinates. CIE  $L^*a^*b^*$  (CIELAB) is a color space specified by the International Commission on Illumination. It describes all the colors visible to the human eye. The three coordinates of CIELAB represent the lightness of the color ( $L^* = 0$  yields black and  $L^* = 100$  indicates diffuse white), its position between red/magenta and green ( $a^*$ , negative values indicate green while positive values indicate magenta) and its position between yellow and blue ( $b^*$ , negative values indicate blue and positive values indicate yellow). Fig 4.2 shows the superpixel segmentation after conversion to lab color space.

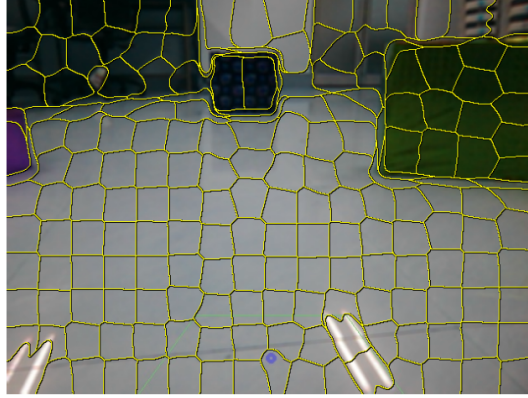


FIGURE 4.2: Superpixel segmentation for K=200 in lab color space.

## 4.2 Gaussian Kernel Smoothing

The image taken by camera is inherently noisy due to errors associated with image acquisition. Gaussian Kernel smoothing technique is used to remove noise from our image before further processing. Width of Gaussian smoothing kernel for pre-processing for each dimension of the image. The same sigma is applied to each dimension in case of a scalar value. The Gaussian kernel in 1D is defined as:

$$K(t) = \frac{1}{\sqrt{2\pi}} e^{-t^2/2} \quad (4.1)$$

After scaling the Gaussian Kernel K by the bandwidth sigma ( $\sigma$ ):

$$K_\sigma(t) = \frac{1}{\sigma} K\left(\frac{t}{\sigma}\right) \quad (4.2)$$

This is the density function of the normal distribution with mean 0 and variance  $\sigma^2$ .

For our experiment we have taken  $\sigma$  value as 5. The n-dimensional isotropic Gaussian kernel is defined as the product of n 1D kernels. Let  $t = (t_1, \dots, t_n)' \in \mathbb{R}^n$ . Then the n-dimensional kernel is given by:

$$K_\sigma(t) = K_\sigma(t_1)K_\sigma(t_2)K_\sigma(t_3)\dots K_\sigma(t_n) \quad (4.3)$$

$$= \frac{1}{(2\pi)^{n/2}\sigma^n} \exp\left(-\frac{1}{2\sigma^2} \sum_{i=1}^n t_i^2\right) \quad (4.4)$$

Without smoothening:

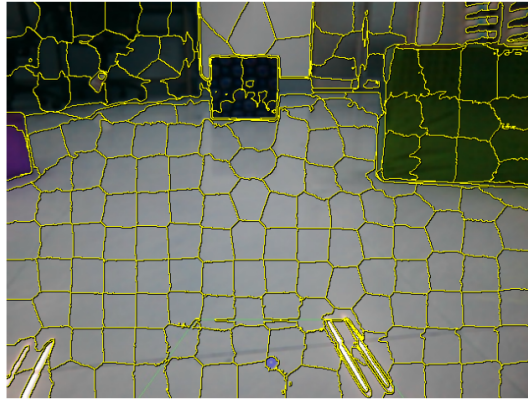


FIGURE 4.3:  $K=200$

After smoothening:

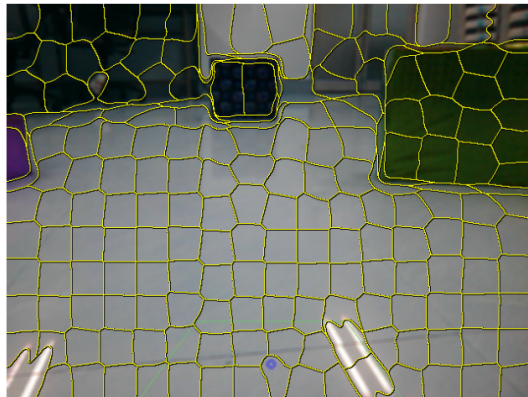


FIGURE 4.4:  $K=200, \sigma=5$

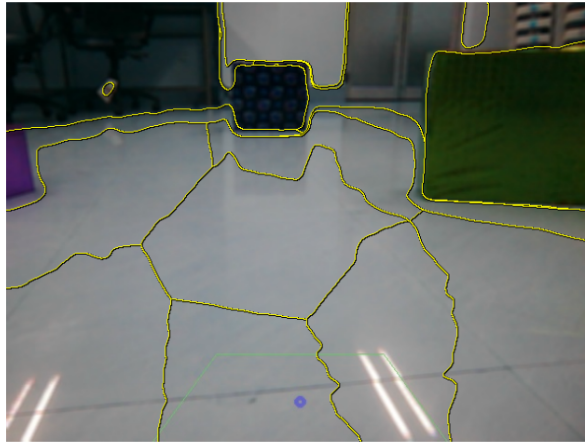
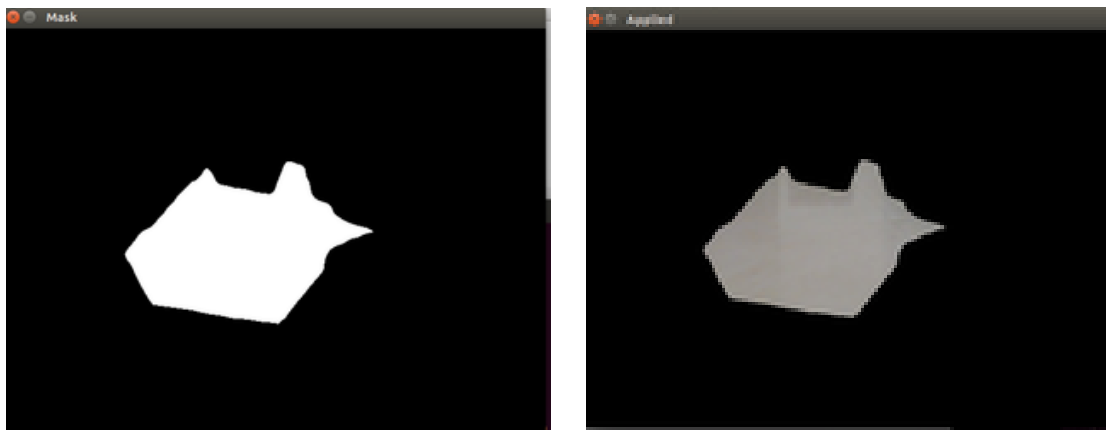
# Histogram Sampling

In our experiment, we have defined safe zone as the region directly in front of the robot that is free of obstacles. We have used a fixed trapezoidal safe zone as shown in Fig 5.1.

Histogram gives us a rough idea of what the rest of the traversable region should look like, because the area directly in front of the robot is generally a good indication of what the rest of the traversable area could look like.

## 5.1 Accessing individual superpixel of segmented image

After applying SLIC superpixel segmentation, we get a 2D segments array of same width and height as the original image. Furthermore, each segment is represented by a unique integer, meaning that pixels belonging to a particular segmentation will all have the same value in the segments array. We construct a mask of the same width and height as the original image and has a default value of 0 (black). By stating `segments = segVal` we find all the indexes, or (x, y) coordinates, in the segments list that have the current segment ID, or `segVal`. We then pass this list of indexes into the mask and set all these indexes to value of 255 (white). Applying these masks we will get individual superpixel which we can use for further processing.

FIGURE 5.1: SLIC superpixel segmentation for  $K=10$ 

(a) Mask

(b) Accessing the corresponding superpixel after applying mask

FIGURE 5.2: Accessing individual pixel after SLIC segmentation for  $K=10$ .

## 5.2 Histogram

The histogram plots the number of pixels in the image (vertical axis) with a particular brightness value (horizontal axis). A histogram represents the distribution of colors in an image [4]. It can be visualized as a graph (or plot) that gives a high-level intuition of the intensity (pixel value) distribution. We are going to assume a RGB color space in this example, so these pixel values will be in the range of 0 to 255.

The RGB histogram is shown in figure:



FIGURE 5.3: Camera Image

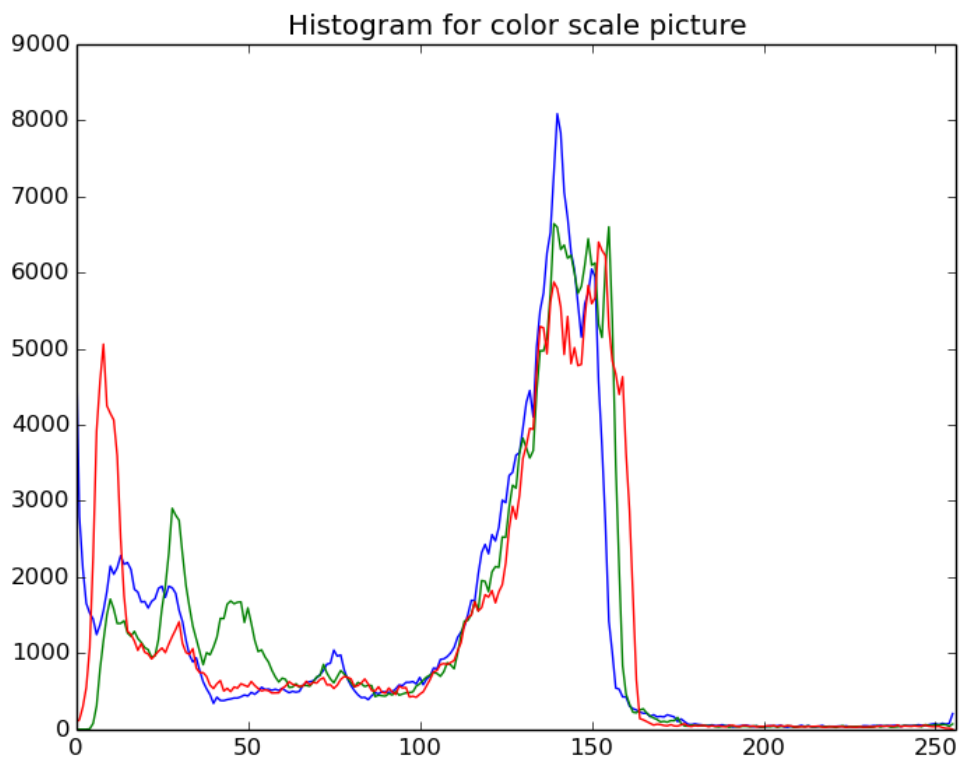


FIGURE 5.4: RGB histogram of camera image

### 5.2.1 Safe zone histogram sampling

For safe zone histogram sampling we use the following algorithm 2.

---

**Algorithm 2** SLIC Superpixel segmentation

---

**Input:** superpixel image, safe zone coordinates

**Output:** BGR histogram

1. Split input image into constituent B, G, R planes.
  2. Create 3 empty histograms: B, G, R.
  3. For each superpixel that has a non-empty intersection with the the safe zone, obtain its B, G and R components and increment the corresponding intensities in the respective histograms.
  4. **return** BGR histogram
- 



FIGURE 5.5: The trapezoidal safe zone, shown in green is used as safe zone.

# Floor Segmentation

Our main aim is to use pixels instead of superpixels to reduce the cost of computation ([5] and [6]). In order to segment the floor from other few observations are made. We start by defining a dependent variable which value will indicate the probability that a superpixel belongs to the floor. The training phase uses the value of this dependent variable for a small set of superpixels that are considered part of the floor.

## 6.1 Calculation of independent Variables

In order to segment the floor from the other objects in an indoor scene we use the following observations:

- We have observed that the shapes of the superpixels area near object boundaries are not regular
- We assume that the superpixels in the safe zone of the images captured by our robot will always correspond to the floor
- The color of the superpixels (i.e., the center pixel in the superpixel area) belonging to the floor should be very similar.
- The shape (bounding box) of the superpixels area that contains pixels with very similar texture tends to be regular, like a square

Using the above observations, following independent parameters are calculated for each superpixel:

- L, a, b channels of superpixels (3 variables)

- actual area of superpixels (1 variable)
- the width, height and diagonals measures of the superpixel area (3 variables)

Therefore a total of 7 independent variables are used for differentiating the floor pixel from others. Previously we have already calculated the superpixel segmented image using SLIC. All the processing and calculations are done in ciela color space. (L, a, b) channel values of each superpixel centers is calculated by iteration. Actual area will be proportional to total number of pixels in one superpixel. Width and height are calculated by noting the maximum horizontal and vertical perpendicular distance from center, i.e number of pixels in both direction with same label. Similarly, length of diagonal is calculated by traversing 45 degree in both direction from center and summing the number of pixels with same label.



FIGURE 6.1: Camera Image

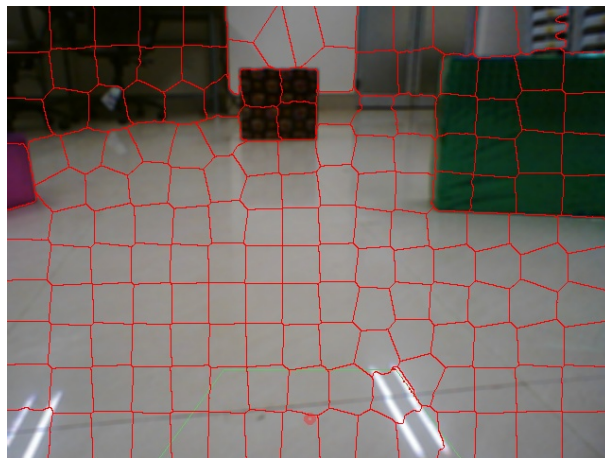


FIGURE 6.2: After applying SLIC for k=200

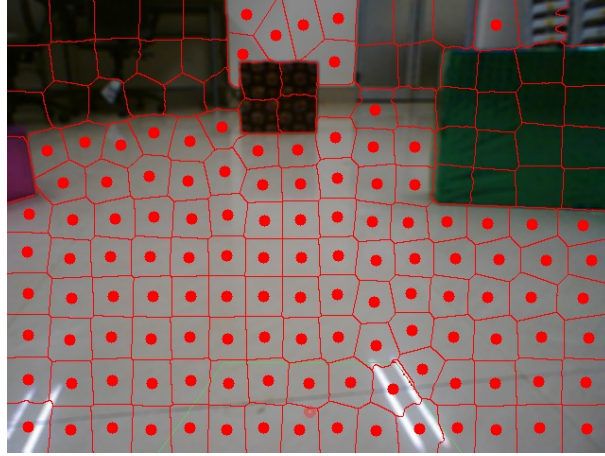


FIGURE 6.3: After applying floor segmentation

## 6.2 Classification of Superpixel

We use a normalized SSD(Sum of Squared Difference) measure to classify if a superpixel belongs to the floor or not. We first compute the mean values for each independent variable of the superpixels in the training set. Then these mean values are subtracted from each independent variable in a superpixel to classify. For the classification, we define a threshold value according to the maximum normalized SSD measure obtained from the training set. For (width, height, diagonal,  $l$ ,  $a$ ,  $b$ , area) as  $(a, b, c, d, e, f, g)$  in every superpixel we calculate:

$$ssd = (a - a_{mean})^2 + (b - b_{mean})^2 + (c - c_{mean})^2 + (d - d_{mean})^2 + (e - e_{mean})^2 + (f - f_{mean})^2 + (g - g_{mean})^2$$

---

**Algorithm 3** SLIC based floor segmentation (image):

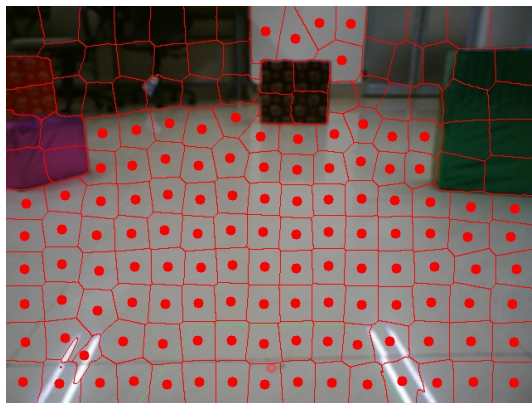
---

1. Convert the image in Lab space.
  2. Perform SLIC on image.
  3. For every superpixel calculate all 7 parameters.
  4. Find the set of superpixel coinciding with safe zone of image.
  5. For coinciding superpixels, find the mean value of all 7 parameters.
  6. Subtract the mean value of each parameter from each superpixel's parameter value.
  7. Find sum of squared difference calculated above.
  8. Using the safe zone superpixels, find the threshold value.
  9. Compare the ssd value of each superpixel with threshold value and categorize as them as floor and non-floor.
- 

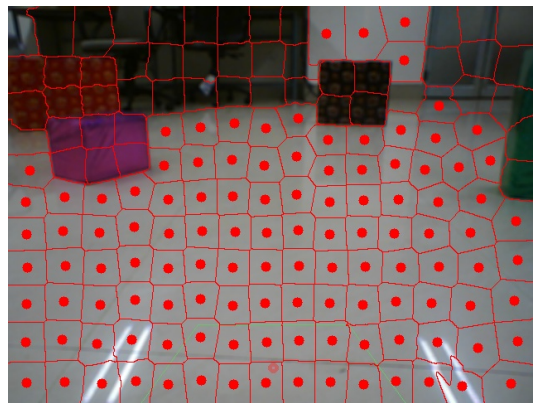
### 6.2.1 Experimental Results

Since we require real-time navigation, we focus mainly on reducing as much as possible the computational time of our segmentation algorithm while keeping its robustness. The computational time for 480 x 640 image is approximately 5 seconds. First, we analyze the effect of using the CIE Lab color space in our classification since this is the color space the SLIC superpixels use. We note that false changes in intensity caused by peculiarities in the floor are kept mostly by the luminance (L) channel. These peculiarities are present due to illumination conditions and properties of the floor itself.

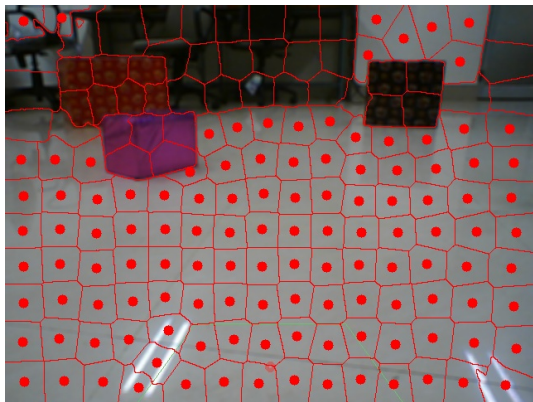
Superpixels with a red dot in its center indicate that all pixels in their area belongs to the floor while superpixels with a no dot are considered as no-floor. Figure 5 shows a set of different indoor images. Our approach achieves nearly 90% detection of free space on the images in our database. The segmentation is good even on highly textured floors and when specularities are present.



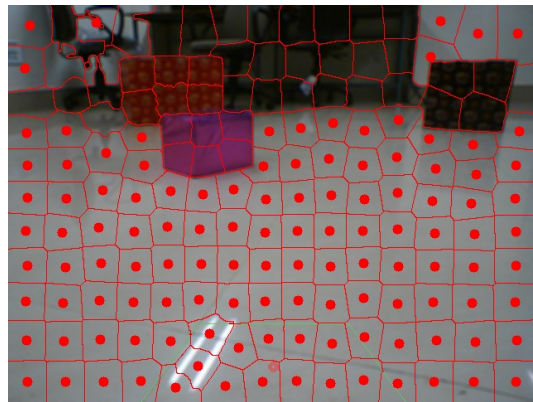
(a)



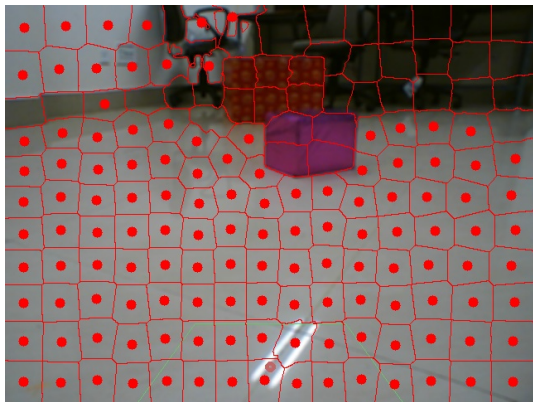
(b)



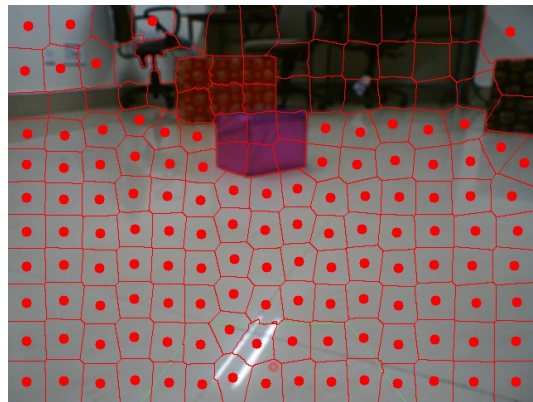
(c)



(d)



(e)



(f)

FIGURE 6.4: Applying floor segmentation on different images.

### 6.3 Problem

The superpixels of walls of room having the same texture as that of floor are marked as floor. We have ignored the fact that the upper region of the image are less probable to be part of the floor and have not used the superpixel center coordinates while computing SSD. This problem is tackled later by using hough lines to find the walls.

### 6.4 Conclusions

We have demonstrated that with only one monocular camera and low resolution images the detection of free space can be robustly achieved. Our approach uses the SLIC superpixels to initially segment the input low resolution image and a normalized SSD similarity measure to classify superpixels that belongs to the floor (free space). The results shown that even with specular reflections, shadows coming from far located objects, and small objects on the floor, our method efficiently segments the free space.

### 6.5 Other floor segmentation methods

Flood fill, also called seed fill, is an algorithm that determines the area connected to a given node in a multi-dimensional array. The flood-fill algorithm takes three parameters: a start node, a target color, and a replacement color. The algorithm looks for all nodes in the array that are connected to the start node by a path of the target color and changes them to the replacement color. There are many ways in which the flood-fill algorithm can be structured, but they all make use of a queue or stack data structure, explicitly or implicitly. The main problem with this method is that it is pixel based computation also the varying illumination condition is not handled. The results are shown in Fig 5.5. Seed is marked as red color circle in safe zone of camera image in Fig 5.1.

---

**Algorithm 4** Flood-fill (node, target-color, replacement-color):

---

1. If target-color is equal to replacement-color, return.
  2. If the color of node is not equal to target-color, return.
  3. Set the color of node to replacement-color.
  4. Perform Flood-fill (one step to the south of node, target-color, replacement-color).
  5. Perform Flood-fill (one step to the north of node, target-color, replacement-color).
  6. Perform Flood-fill (one step to the west of node, target-color, replacement-color).
  7. Perform Flood-fill (one step to the east of node, target-color, replacement-color).
  8. Return.
- 

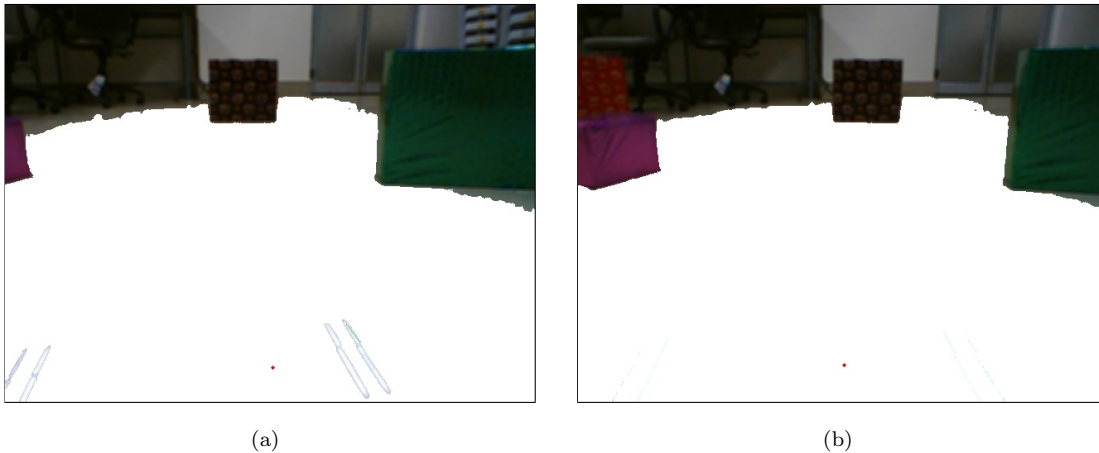


FIGURE 6.5: Applying Flood fill on different images.

## 6.6 Floor Junction Masking

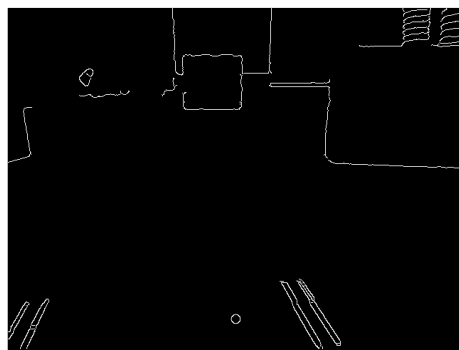
We have seen the problems faced while floor segmentation due to wall superpixels. So in order to further improve the occupancy image, this algorithm detects probable floor junctions using Canny Edge Detection, contour detection using Suzuki85 algorithm and the Probabilistic Hough Line transform to mask the image, and get even better results. The key is using vertical lines as possible edges of walls/obstacles, since vertical lines remain vertical (invariant) no matter how the robot is oriented (keeping in mind the stated assumptions) whereas this is not the case with horizontal lines. For each of the

detected vertical lines, the algorithm estimates where it meets the floor by finding the non-vertical lines that lie within a threshold radius from the bottom of the vertical line under consideration. Accordingly, it masks the corresponding region in the occupancy map. The approach is outlined in following Algorithm.

Note that this stage operates directly on the smoothed camera image, not on the super-pixels. The mask produced by Algorithm is ANDed with the occupancy image produced by previous algorithms applied in succession to give the final result.



(a)



(b)

FIGURE 6.6: Applying Canny edge detection

---

**Algorithm 5** Floor Junction Masking

---

**Input:** camera image **Output:** binary occupancy mask

1. Init occupancy mask  $m \leftarrow$  WHITE for all pixels.
  2. Init floor junctions list  $F J \leftarrow \{\}$ .
  3. Convert input image from BGR  $\rightarrow$  Grayscale.
  4. Detect edges  $E$  in input image use Canny edge detection.
  5. Detect contours  $C$  from  $E$  using Suzuki85 algorithm.
  6. Obtain lines  $L$  from  $C$  using Probabilistic Hough Transform.
  7. **for all** vertical lines  $vl$  in  $L$  **do**
  8.     **for all** non-vertical lines  $fl$  in  $L$  **do**
  9.         **iff**  $l$  lies within circle of threshold radius from bottom of  $vl$  **then**
  10.              $F J.add((vl, fl))$
  11.         **end if**
  12.     **end for**
  13. **end for**
-

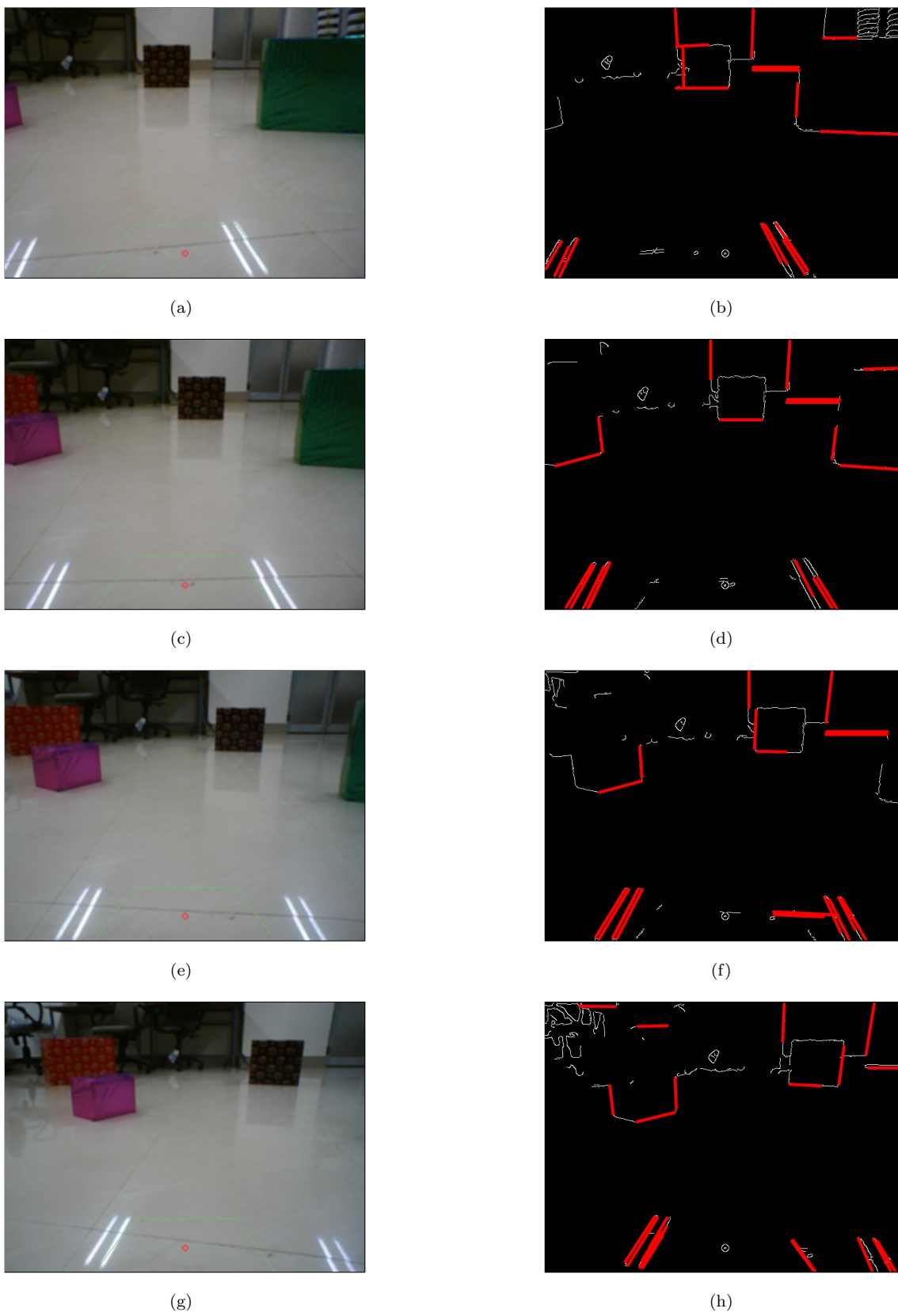


FIGURE 6.7: Applying Hough line transform

## 6.7 Region Growing

Once we get the superpixel segmented region, we apply the region growing to get the floor part only. We define the seed point as the centroid of the safe zone. It is shown in red in Fig. 5.6a. From the superpixel containing the seed point, we run a breadth first search over the superpixels. We maintain a set of superpixels called the traversable set, which contains all the regions that have been detected as belonging to the floor. In the BFS, we consider the 4-neighbors of a superpixel in the traversable set frontier. We add a neighbor to the traversable set, if the threshold value discussed before is satisfied. The steps are outlined below.

---

### Algorithm 6 Region Growing

---

**Input:** superpixel image, threshold value, seed point, *ssd* **Output:** binary occupancy mask

1. queue  $Q \leftarrow$  seed superpixel.
  2. occupancy image  $occ \leftarrow$  BLACK for all superpixels.
  3. Convert input image from BGR  $\rightarrow$  Grayscale.
  4. **while**  $Q$  is not empty **do**
  5.     Superpixel  $sp \leftarrow$  dequeue( $Q$ )
  6.     **for all** unvisited 4-nbbrs of  $sp$  **do**
  7.         **if**  $ssd \leq$  threshold
  8.             **then**
  9.                  $Q \leftarrow$  enqueue( $nbr$ )
  10.                  $occ[nbr] \leftarrow$  WHITE
  11.             **end if**
  12.     **end for**
  13. **end while**
  14. **return**  $occ$
-

## 6.8 Results



(a)



(b)

FIGURE 6.8: After applying Region Growing

# Mapping the environment

## 7.1 Overview

So far in this report, we have seen how to distinguish obstacles from the traversal region just by using monocular vision. The output of this is a binary occupancy image. Once a robot can detect obstacles and navigate reliably, it needs to construct a map of its environment. Most of the well-established techniques, such as occupancy grids, rely on range data. This data is in the form of radial distance and angle measurements to the obstacles relative to the position of the robot. However, for monocular vision, we need to use a different approach to calculate the range information, since it is not readily available. The goal of the personal robot is to dynamically create a map of the unstructured environment that it has been placed. Having identified the obstacles in the previous section, placing them on the map requires a transformation from the image coordinate space to the real world coordinate space. In this section, we describe a method to convert from image plane to ground plane. This is in contrast to many monocular approaches that create a sparse 3-D map of features in the environment, such as [7] and [8]. This representation is fast, intuitive and more importantly, convenient to work with for subsequent stages, like path-planning. Finally, we present a look up table which can be used for easy transformation.

## 7.2 Perspective Mapping

### 7.2.1 Image Formation and Perspective Mapping

Monocular images are two dimensional and the process of capturing an image loses the depth information and introduces a perspective mapping, since all the points in the 3-D space along a ray of light traced from the camera lens will map to the same pixel in the

image. Since obstacles are present in the environment, occlusion prevents the camera from seeing past the nearest obstacle along the ray. Inverse perspective mapping (IPM) is a method for turning an image back into a 3-D map, i.e. it tries to reverse the effect of the perspective mapping. It involves an analysis based on homogeneous coordinates and perspective transformation matrix.

## 7.2.2 Homogeneous Coordinates

Homogeneous coordinates are simply a way of representing  $N$ -dimensional coordinates with  $N + 1$  numbers, i.e. the point  $(x;y)$  in the Cartesian system becomes  $(X;Y;w)$  in homogeneous coordinate system, where  $w$  is an additional variable. Homogeneous coordinates allow affine transformations (translation, scaling, shearing, rotation etc.) to be easily represented using matrix operations.

## 7.2.3 Homography

One of the uses of homogenous coordinates is in homography. A homography is a transformation (matrix) from one plane to another. Two images are related by a homography if and only if both images are viewing the same plane from a different angle. IPM is thus a homography, as shown in Fig. 6.1 .

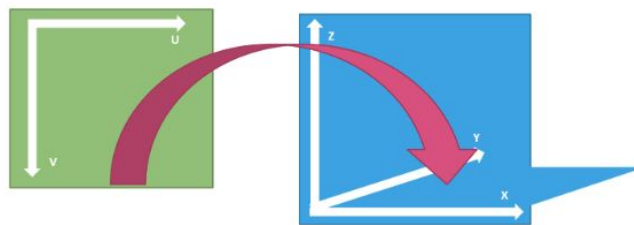


FIGURE 7.1: Coordinate convention for camera image space (left) and ground space (right)

For analysis, we make the assumption that our camera is an idealized pinhole camera, which suits for most applications. In that case, the camera matrix, which describes the mapping from 3D points in the world to 2D points in an image, depends only on the focal length of the camera. So, if we knew the focal length, then we could easily and this transformation matrix. However, in general for a digital camera, the focal length is unknown. Thus we use another method to estimate the distance using IPM, detailed in the next section.

### 7.3 Algorithm

The homography is calculated using 4 point correspondence, giving us all the information to transform between image plane and ground plane coordinates. Limitation of this approach is that it assumes a uniformly parametrized image plane (pinhole camera), so lens distortion will give us errors as seen in my example. If we are able to remove lens distortion effects, we'll go very well with this approach. In addition we will get some error of giving slightly wrong pixel coordinates as our correspondences, we can get more stable values if you provide more correspondences. Using this input image shown in Fig 6.2.



FIGURE 7.2: Input Image for mapping

The four corners of one chess field are read from mouse click, which will correspond to the fact that we know 4 points in our image. Points are marked red in the following image.



FIGURE 7.3: Corners of chess field

We define 4 points representing our top-down view of the image. The first entry in the list is  $(0, 0)$  indicating the top-left corner. The second entry is  $(\text{maxWidth} - 1, 0)$  which corresponds to the top-right corner. Then we have  $(\text{maxWidth} - 1, \text{maxHeight} - 1)$  which is the bottom-right corner. Finally, we have  $(0, \text{maxHeight} - 1)$  which is the bottom-left corner.

The takeaway here is that these points are defined in a consistent ordering representation and will allow us to obtain the top-down view of the image. To actually obtain the top-down, birds eye view of the image we will utilize the perspective transformation discussed before. For transformation we require the 4 ROI points in the original image and a list of transformed points and we can calculate the transformation matrix  $M$  using that. Applying the transformation matrix we get our warped image which is our top-down view. In this image the corner of chess fields are marked.



FIGURE 7.4: Warped Image



FIGURE 7.5: Input Image for mapping

We can see there is some big amount of error in the data. as said before it's because of slightly wrong pixel coordinates given as correspondences (and within a small area!) and because of lens distortion preventing the ground plane to appear as a real plane on the image. The lookup table is calculated in the same manner for every corners.

Error is calculated using sum of squared difference of the two corresponding points.

## 7.4 Test Platform

Our test robot is shown in Fig. 6.6. We have used a Sony Playstation Eye USB webcam as our sensor, an Arduino Uno as our microcontroller, and a standard laptop processor. The robot is equipped with a differential drive mechanism and is powered by a 12 V battery pack. The OpenCV library, developed by Intel, has been used to prototype and test our algorithms.



FIGURE 7.6: Test robot

# Future Work

Future work which can be carried on are as follows:

- Probabilistic occupancy grid generation

SLAM algorithm can be combined with an exploration procedure. Exploration strategy should be able to cover the unknown terrain as fast as possible avoiding repetition as much as possible but this is suboptimal in the context of slam because the robot typically needs to re-visit places to localize itself. There are two standard methods [9] and [10] which can be used for generating probability occupancy grid. Using the frontier mapping, we need to estimate the best possible direction.

# Conclusion

In this project, we developed methods to develop some of the building blocks for autonomous robot navigation using monocular vision. We are working on a multi-stage obstacle detection technique based on monocular vision which has its own advantages and disadvantages. We are using computationally fast algorithm for each step hence reducing the complexity. But on the other hand it has a constraint that it cannot be used in low light situation due to sensor limitations.

Obstacle detection and avoidance in real time is a complex and computationally expensive. We have used a novel  $O(N)$  complexity superpixel segmentation algorithm that is simple to implement and outputs better quality superpixels for a very low computational and memory cost. It needs only the number of desired superpixels as the input parameter. It scales up linearly in computational cost and memory usage. Using the superpixel segmentation method a complete map of the traversal region is created which will be used for exploration. The problem now lies in developing the best strategy for exploration. After detecting the obstacles, we will be able to generate potential destinations and along with the occupancy map, we will be able to explore the entire region.

In conclusion, this project has shown that the simple webcam which is easily available to everyone can be used for indoor robot navigation, reducing the complexity and computation cost. Thus, this approach is of industrial importance thereby simplifying the daily life needs.

# Bibliography

- [1] A. Pant, “Mapping the environment, thesis on ”towards a personal assistant robot using monocular vision,” in *IIT Kharagpur Thesis*, 2015.
- [2] S. Riisgaard and M. Blas, “A tutorial approach to simultaneous localization and mapping,” *Massachusetts Institute of Technology (MIT), Mobile Robotics course materials*, 2012.
- [3] R. Achanta, A. Shaji, K. Smith, A. Lucchi, P. Fua, and S. Süsstrunk, “Slic superpixels compared to state-of-the-art superpixel methods,” *IEEE transactions on pattern analysis and machine intelligence*, vol. 34, no. 11, pp. 2274–2282, 2012.
- [4] A. Mobarhani, S. Nazari, A. H. Tamjidi, and H. D. Taghirad, “Histogram based frontier exploration,” in *Intelligent Robots and Systems (IROS), 2011 IEEE/RSJ International Conference on*, pp. 1128–1133, IEEE, 2011.
- [5] S. Kumar, A. Dewan, and K. M. Krishna, “A bayes filter based adaptive floor segmentation with homography and appearance cues,” in *Proceedings of the Eighth Indian Conference on Computer Vision, Graphics and Image Processing*, p. 54, ACM, 2012.
- [6] F. G. Rodriguez-Telles, L. A. T. Mendez, and E. A. M. Garcia, “A fast floor segmentation algorithm for visual-based robot navigation,” in *Computer and Robot Vision (CRV), 2013 International Conference on*, pp. 167–173, IEEE, 2013.
- [7] B. Yamauchi, “A frontier-based approach for autonomous exploration,” in *Computational Intelligence in Robotics and Automation, 1997. CIRA’97., Proceedings., 1997 IEEE International Symposium on*, pp. 146–151, IEEE, 1997.
- [8] K. Wnuk, F. Dang, and Z. Dodds, “Dense 3d mapping with monocular vision,” in *Proceedings of the 2nd International Conference on Autonomous Robots and Agents (ICARA04)*, 2004.

- 
- [9] A. J. Davison, I. D. Reid, N. D. Molton, and O. Stasse, “Monoslam: Real-time single camera slam,” *IEEE transactions on pattern analysis and machine intelligence*, vol. 29, no. 6, pp. 1052–1067, 2007.
- [10] Y. Wang, A. Liang, and H. Guan, “Frontier-based multi-robot map exploration using particle swarm optimization,” in *Swarm Intelligence (SIS), 2011 IEEE Symposium on*, pp. 1–6, IEEE, 2011.